0026-895X/06/7001-16–22$20.00
MOLECULAR PHARMACOLOGY
Copyright © 2006 The American Society for Pharmacology and Experimental Therapeutics
Mol Pharmacol 70:16–22, 2006

Vol. 70, No. 1
23259/3116044
Printed in U.S.A.

Role of the Outer β-Sheet in Divalent Cation Modulation of α7 Nicotinic Receptors

James T. McLaughlin, Jie Fu, Adrian D. Sproul,[1] and Robert L. Rosenberg

Departments of Pharmacology (J.T.M., J.F., A.D.S., R.L.R.) and Cell & Molecular Physiology (R.L.R.), University of North Carolina at Chapel Hill, Chapel Hill, North Carolina

Received February 7, 2006; accepted March 13, 2006

ABSTRACT

α-7 Nicotinic acetylcholine receptors (AChRs) exhibit a positive modulation by divalent cations similar to that observed in other AChRs. In the chick α7 AChR, this modulation involves a conserved glutamate in loop 9 (Glu^{172}) that undergoes agonist-dependent movements during activation. From these observations, we hypothesized that movements of the nearby β-sheet formed by the β7, β9, and β10 strands may be involved in agonist activation and/or divalent modulation. To test this hypothesis, we examined functional properties of cysteine mutations of the β7 and β10 strands, alone or in pairs. We postulated that reduced flexibility or mobility of the β7/β9/β10-sheet as a result of introduction of a disulfide bond between the β strands would alter activation by agonists. Using a nondesensitizing α7 mutant background ($L^{247}T$), we identified one mutant pair, $K^{144}C + T^{198}C$, that exhibited a unique characteristic: it was fully activated by divalent cations (Ca^{2+}, Ba^{2+}, or Sr^{2+}) in the absence of acetylcholine (ACh). Divalent-evoked currents were blocked by the α7 antagonist methyllycaconitine and were abolished when Glu^{172} was mutated to glutamine. When the $K^{144}C + T^{198}C$ pair was expressed in wild-type α7 receptors, activation required both ACh and divalent cations. We conclude that the introduction of a disulfide bond into β7/β9/β10 lowers the energetic barrier between open and closed conformations, probably by reducing the torsional flexibility of the β-sheet. In this setting, divalent cations, acting at the conserved glutamate in loop 9, act as full agonists or requisite coagonists.

Nicotinic acetylcholine receptors are members of the cysteine-loop family of receptors which transduce the energy of ligand binding into protein conformational changes that result in the opening of a transmembrane ion channel (Karlin, 2002). All of the genes in this family encode bifunctional polypeptides featuring an extracellular ligand binding domain (LBD) fused to a transmembrane ion channel domain (ICD). Functional receptors are composed of homologous or identical polypeptides assembled as a pentamer around a central pore. Although there is a wealth of information identifying specific functional regions of both the LBD and the ICD (Sine, 2002; Lester et al., 2004), an explicit coupling mechanism remains to be elucidated.

Our understanding of ligand binding has been advanced greatly by crystal structures of several invertebrate AChbinding proteins (AChBPs; Brejc et al., 2001; Celie et al., 2005a,b). These soluble proteins share sequence homology with the LBD of nicotinic receptor subunits (~24% sequence identity with the α7 subunit), and they assemble as homopentamers around a central cavity. The AChBP contains a core of 10 β-strands, 1 α-helix, and 10 variable regions linking secondary structural elements (Brejc et al., 2001). The β-strands form two major antiparallel sheet structures referred to as the inner (β1, β2, and β6) and outer (β7, β9, and β10) sheets (Unwin, 2005). The structure also displays a clustering of conserved aromatic residues in proximity to both the subunit interface and the loop between β strands 9 and 10 (the "C loop"). Crystal structures of AChBPs in complex with nicotine, carbamoylcholine, or the peptide antagonist α-conotoxin PnIA have identified specific ligand-receptor contacts and confirmed that ligand binding involves the contraction of the C loop (Celie et al., 2005a,b).

Several current models attempt to interpret functional data in terms of possible conformational steps leading from agonist binding and C-loop contraction to channel opening. In one model, agonist binding leads to a rotation of the inner β-sheet of one or more subunits, followed by similar movement of the second-channel transmembrane domain (M2) (Horenstein et al., 2001; Unwin, 2005). A "conformational

Supported by National Institute on Drug Abuse grant DA017882 (to R.L.R.).
[1] Current affiliation: Department of Cell and Molecular Biology, Medical University of South Carolina, Charleston, South Carolina.
Article, publication date, and citation information can be found at http://molpharm.aspetjournals.org.
doi:10.1124/mol.106.023259.

ABBREVIATIONS: LBD, ligand-binding domain; ACh, acetylcholine; AChR, nicotinic acetylcholine receptor; ICD, ion channel domain; MTSET, 2-trimethylammonioethylmethane thiosulfonate; ESLC, extracellular recording solution containing low Ca^{2+} concentration; ND96, *X. laevis* oocyte storage buffer; MLA, methyllycaconitine; AChBP, acetylcholine binding protein; BSA, bovine serum albumin.

wave" theory suggests that these or similar steps occur in sequential order from LBD domain to ICD domain (Grosman et al., 2000). More explicit models link agonist binding to channel opening via interactions between several pairs of residues (Lee and Sine, 2005; Mukhtasimova et al., 2005). In these models, electrostatic or hydrogen bonds between residues in the C-loop, the outer β-sheet, and the inner β-sheet propagate the signal of agonist binding to the interface between the LBD and the transmembrane helices that form the ICD. They provide a more detailed description of mechanisms proposed previously of coupling between binding and channel gating (Miyazawa et al., 2003) and are similar to a model proposed for activation of the related $GABA_A$ receptor (Kash et al., 2004).

Our approach to examining receptor activation pathways uses cysteine scanning to track conformational changes based on rates of thiol modification (Karlin and Akabas, 1998). We demonstrated that a region of the α7 AChR known to be involved in modulation by divalent cations, loop 9, undergoes agonist-dependent conformational movements (Lyford et al., 2003). Based on this result and on our homology model of the α7 LBD, we postulated that a disulfide bond between β strands would reduce the flexibility or mobility of the outer (β7/β9/β10) sheet and could lead to alterations in receptor activation. If movements of the receptor around Glu^{172} (in loop 9) induced by agonist are due to global movements of the outer β-sheet, then an introduced disulfide should have a significant effect on activation.

In this report, we test this idea by examining the effect of introduced disulfide bonds between the β7 and β10 strands. We used our homology model of the α7 extracellular domain to identify sites for disulfide engineering, selecting residues with the β carbons separated by an appropriate distance for disulfide formation (<6 Å). Using this criterion, Asn^{142} was paired with Thr^{198} and Thr^{200}, whereas Lys^{144} was paired with Asp^{196} and Thr^{198}. Several additional pairs that were predicted to be too distant to form a disulfide (Asn^{142}/T^{202} and Lys^{144}/Thr^{200}) were also included. We examined functional properties of both single cysteine mutations and paired mutations using a nondesensitizing AChR background ($L^{247}T$) (Eddins et al., 2002a,b; Lyford et al., 2003). The unique phenotype of one pair, α7-$K^{144}C$/$T^{198}C$, confirmed the importance of the outer β-sheet in the coupling of agonist binding to channel opening and suggested that cholinergic agonists and divalent cations initiate similar conformational transitions in the process of receptor activation.

Materials and Methods

Reagents. Ethyl trimethyl methane thiosulfonate (MTSET) was obtained from Toronto Research Chemical (Toronto, ON, Canada). Gentamicin was from Invitrogen (Carlsbad, CA). All other reagents were obtained from either Fluka (Ronkonkoma, NY) or Sigma (St. Louis, MO).

Site-Directed Mutagenesis. We used an α7 receptor containing two mutations ($C^{115}A$, $L^{247}T$) as our "background" for mutations described in this study. We mutated the lone unpaired cysteine in the extracellular domain (Cys^{115}) to allow more straightforward interpretation of MTSET exposure experiments. We observed no functional effect of this mutation on receptor expression or ACh response. We included the mutation in the M2 transmembrane domain leucine 247 ($L^{247}T$; L9′T) because of its large current amplitudes and nondesensitizing kinetics compared with wild-type α7 receptors (Revah et al., 1991). All mutations were introduced into chick α7 cDNA by site-directed mutagenesis using the QuikChange method (Stratagene, La Jolla, CA) as described previously (Eddins et al., 2002b) and were confirmed by DNA sequencing.

***Xenopus laevis* Oocyte Maintenance and Expression.** Oocytes were surgically removed and prepared from female *X. laevis* in accordance with the University of North Carolina Institutional Animal Care and Use Committee guidelines as described previously (Eddins et al., 2002a). cRNA was prepared using the T7 RNA polymerase and mMessage mMachine kit (Ambion, Austin, TX) as described by the manufacturer. Oocytes were injected with 20 ng of cRNA and incubated at 18°C in ND96 (5 mM HEPES, 96 mM NaCl, 2 mM KCl, 1 mM $MgCl_2$, and 1.8 mM $CaCl_2$, pH 7.5) for 2 to 5 days before use.

Data Collection and Analysis. Oocytes were superfused in normal extracellular solution containing a reduced Ca^{2+} concentration (ESLC; 96 mM NaCl, 2 mM KCl, 1 mM $MgCl_2$, 0.1 mM $CaCl_2$, and 10 mM HEPES, pH 7.5). Two-electrode voltage clamp was performed with a GeneClamp 500B controlled by pCLAMP6 software (Axon Instruments, Sunnyvale, CA). Electrodes were filled with 3 M KCl contacting Ag-AgCl wires and had resistances of 0.5 to 2.0 MΩ. Currents were recorded at a constant holding potential of −60 mV. Currents were low-pass-filtered at 50 or 125 Hz and were sampled at 250 Hz. Agonist dose-response curves were obtained as described previously (Eddins et al., 2002a), and data were fit to the Hill equation using Origin software (OriginLab Corp., Northampton, MA).

Modification by MTSET. MTSET was prepared daily in water and stored on ice. Stock solution was diluted to the appropriate working concentration in ESLC immediately before each application. Oocytes were exposed to MTSET by continuous flow for 15 to 60 s, followed by a 5-min wash. To measure accessibility of each cysteine mutant, currents evoked by a submaximal concentration of ACh were compared before and after MTSET exposure. We also determined complete ACh dose-response relationships before and after MTSET for those mutants which showed sensitivity to the modifier.

Oocyte Antibody Binding Assay. Oocytes injected with cRNA were incubated 2 to 5 days before assay. They were fixed with 2% paraformaldehyde in HEPES-buffered saline (20 mM HEPES and 100 mM NaCl, pH 7.4) for 20 min at 22°C, rinsed with 3 changes of ND96, and then incubated 30 min in ND96 plus 3% BSA. Oocytes were then incubated overnight at 4°C in ND96, 3% BSA, plus a 1:500 dilution of anti-α7 antiserum. The antiserum (Ab1382) was raised in rabbits against a peptide corresponding to the N-terminal sequence of rat α7 AChR (EFQRRLYKELVKNYN). After six washes in ND96, the oocytes were incubated for 2 h at 22°C in ND96/BSA plus 2 nM ^{125}I-labeled goat anti-rabbit IgG (PerkinElmer Life and Analytical Sciences, Boston, MA). After five washes with ND96, bound secondary antibody was determined using a gamma counter. Nonspecific binding was measured to either uninjected oocytes or to injected oocytes incubated with primary antibody preincubated with excess antigenic peptide.

Structural Model of α7. A model of the chick α7 nicotinic receptor extracellular domain based on the coordinates of the *Lymnea* ACh binding protein was constructed as described previously (Lyford et al., 2003). Images of the model were generated using an open-source version of Pymol (DeLano Scientific, South San Francisco, CA).

Results

Single Cysteine Mutations in β7 and β10 Are Well-Tolerated. Our model of the chick α7 LBD suggests that the side chain of Asn^{142} is positioned in close proximity to those of Thr^{198} and Thr^{200}. Likewise, Lys^{144} is positioned near Asp^{196} and Thr^{198}. The distance between β-carbons of each of these pairs is ~4.5 Å (Fig. 1). These five residues (and Thr^{202})

were mutated individually to cysteine and tested for functional expression in *X. laevis* oocytes. Table 1 shows a summary of the dose-response data for these mutations. Five of the six substitutions caused modest rightward shifts in the acetylcholine dose-response curve relative to the parent genotype, $C^{115}A/L^{247}T$. Only the $K^{144}C$ mutant caused an increase of more than ~6-fold in the ACh EC_{50} values. Peak currents for each mutant were also comparable with those measured in $C^{115}A/L^{247}T$ α7 AChRs.

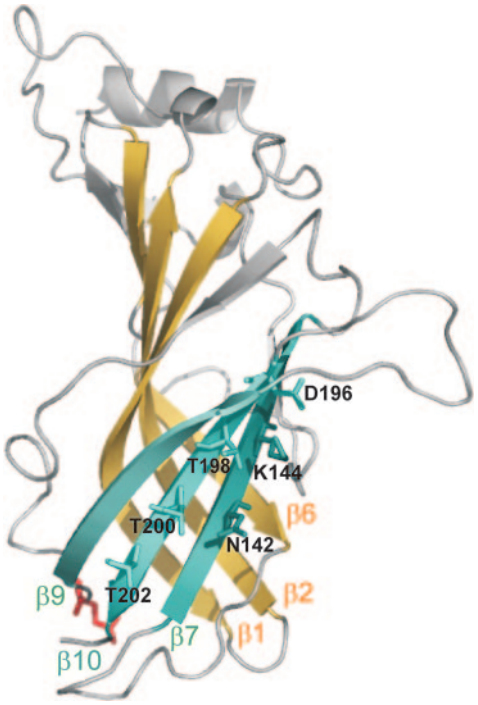

Fig. 1. Structural model of an α7 subunit (from Eddins et al., 2002). The sequence is depicted as two major regions defined by inner and outer β-sheets. The inner β-sheet (β1, β2, and β6) is shown in yellow. The outer β-sheet is shown in blue (β7, β9, and β10). Residues used in disulfide engineering are highlighted with native side chains superimposed over ribbon figure. These include Asn^{142} and Lys^{144} in the β7 strand and Asp^{196}, Thr^{198}, Thr^{200}, and Thr^{202} in β10. The conserved glutamate essential for modulation by divalent cations, Glu^{172}, is shown in red. This model is based on the HEPES-bound conformation of the AChBP (Brejc et al., 2001) and thus is likely to represent an activated or desensitized conformation.

We examined the solvent accessibility of the introduced cysteines by measuring ACh responses before and after exposure to the thiol modifier MTSET. Both $N^{142}C$ and $K^{144}C$ displayed significant leftward shifts in their ACh dose-response profiles, demonstrating that both introduced cysteines were accessible to the modifying agent. MTSET also had a significant effect on $D^{196}C$, causing a ~70-fold increase in the EC_{50} value of ACh. In a previous study involving cysteine substitution of this conserved aspartate in the *Torpedo californica* AChR, modification caused either inhibition or constitutive activation depending on the specific modifier used (Sullivan and Cohen, 2000). Exposure of $T^{198}C$ or $T^{200}C$ to MTSET caused consistent shifts in the ACh dose-response curves, but these did not reach the level of statistical significance. We conclude that $N^{142}C$, $K^{144}C$, and $D^{196}C$ are clearly accessible to the surrounding aqueous solvent.

Functional α7 Receptors Are Formed by Select Pairs of Cysteine Mutants. We next constructed and tested six mutant pairs designed to position cysteines in close proximity in the β7 and β10 strands. Each of the β7 cysteine replacements was paired with three cysteine substitutions in β10; the model predicts that, in each case, at least two of these three pairs should be close enough to form a disulfide bond. We found that only two of the pairs, $N^{142}C/T^{200}C$ and $K^{144}C/T^{198}C$, form ACh-responsive channels when expressed in oocytes. ACh dose-response profiles of these mutants are shown in Fig. 2. Both double-mutant pairs displayed leftward shifts in the ACh EC_{50} values relative to one or both of their respective single-mutant parental genotypes, suggesting some degree of phenotypic rescue.

As a test for disulfide formation, we examined the effect of thiol modification on ACh-evoked currents in both mutant pairs. MTSET modification is specific for free thiols and has no effect on disulfides (Holmgren et al., 1996); MTSET exposure caused a statistically significant decrease in the ACh EC_{50} values of both $N^{142}C$ and $K^{144}C$ single mutants (Table 1). Yet when these two mutations were expressed paired with a second cysteine ($T^{200}C$ or $T^{198}C$, respectively), sensitivity to MTSET was lost (Table 1). These observations suggest that

TABLE 1

Properties of cysteine mutants

Values in parentheses represent the number of determinations for each measure. Efficacy measure is a percentage of maximal ACh-evoked current elicited by 10 mM Ba^{2+}.

	EC_{50} ACh	Post-MTSET EC_{50}	ΔMTSET	I_{max} ACh	Ba^{2+} Efficacy	Surface Expression (IgG Binding)
	μM	*μM*		*μA*	*%*	*fmol/oocyte*
$C^{115}A + L^{247}T$	2.44 ± 0.14 (7)	1.91 ± 0.11 (4)	N.E.	6.31 ± 0.9	12 (9)	5.29 ± 0.78 (7)
$N^{142}C$	8.49 ± 0.38 (8)	5.94 ± 0.35 (8)*	↓ EC_{50}	2.30 ± 0.8	0.8 (6)	N.D.
$K^{144}C$	112.2 ± 7.8 (7)	79.4 ± 4.9 (7)*	↓ EC_{50}	0.71 ± 0.3	0.9 (9)	N.D.
$D^{196}C$	15.7 ± 0.6 (6)	1067 ± 171 (5)*	↑ EC_{50}	5.90 ± 0.3	5.5 (4)	N.D.
$T^{198}C$	6.98 ± 0.50 (6)	5.86 ± 0.5 (5)	N.E.	0.34 ± 0.9	3.8 (6)	N.D.
$T^{200}C$	5.83 ± 0.48 (6)	4.65 ± 0.9 (5)	N.E.	2.04 ± 1.5	0.8 (5)	N.D.
$T^{202}C$	3.60 ± 0.86 (5)	3.63 ± 0.32 (3)	N.E.	4.67 ± 2.2	2.3 (3)	N.D.
$N^{142}C/T^{198}C$	N.R.	N.D.	N.D.	N.D.	N.D.	3.01 ± 0.33 (6)
$N^{142}C/T^{200}C$	2.29 ± 0.3 (6)	2.13 ± 0.24 (4)	N.E.	7.0 ± 1.3 (6)	15 (5)	1.46 ± 0.15 (4)
$N^{142}C/T^{202}C$	N.R.	N.D.	N.D.	N.D.	N.D.	1.73 ± 0.24 (3)
$K^{144}C/D^{196}C$	N.R.	N.D.	N.D.	N.D.	N.D.	6.90 ± 0.93 (4)
$K^{144}C/T^{198}C$	10.5 ± 1.4 (7)	9.25 ± 1.13 (6)	N.E.	8.1 ± 1.0 (6)	96 (6)	1.34 ± 0.34 (4)
$K^{144}C/T^{200}C$	N.R.	N.D.	N.D.	N.D.	N.D.	1.02 ± 0.37 (7)
$K^{144}C/T^{198}C/E^{172}Q$	531 ± 11 (7)	N.D.	N.D.	5.5 ± 1.4 (7)	0 (9)	N.D.
$K^{144}C/T^{198}C + L^{247}L$	478 ± 38 (5)	N.D.	N.D.	0.44 ± 0.21 (5)	N.D.	N.D.

N.D., not determined; N.E., no effect; N.R., no response to ACh.
* Statistically significant from EC_{50} values pre-MTSET at $P < 0.05$ using paired t test.

disulfide bonds were formed between introduced cysteines in both the $N^{142}C/T^{200}C$ pair and the $K^{144}C/T^{198}C$ pair.

The absence of functional receptors in four of six mutant pairs may be due to an interaction between the introduced cysteines that prevented ACh-evoked activation. On the other hand, it may have resulted from a perturbation in receptor translation, folding, assembly, or surface expression. To determine whether nonfunctional receptors containing cysteine pairs were expressed on the oocyte surface, we used an antibody binding assay (Table 1). All six of the mutant pairs expressed measurable surface antibody binding (1–10 fmol of antibody binding sites per oocyte). This indicates that the lack of ACh responsiveness in four of the six pairs of introduced cysteines was not caused by a defect in surface expression. For those cysteine pairs unresponsive to agonist, therefore, the specific combinations of mutations seem to disrupt agonist binding and/or receptor gating.

$K^{144}C/T^{198}C$ α7 AChRs Are Activated by Both ACh and Divalent Cations. In our initial characterization of the $K^{144}C/T^{198}C$ mutant, we observed basal currents in the absence of agonist that were higher than normal. These early experiments used a physiological Ca^{2+} concentration (1.8 mM). The basal currents were eliminated when we used a low-calcium (0.1 mM) extracellular recording solution (ESLC). Ba^{2+}, Ca^{2+}, or Sr^{2+} activated an inward current only in oocytes expressing the $K^{144}C/T^{198}C$ α7 AChR. We measured the dose-response relationship for Ba^{2+}-evoked current and found that maximal currents were similar in magnitude to those elicited by ACh (Fig. 3A). Currents elicited by Ca^{2+} or Sr^{2+} (data not shown) were similar to those observed when Ba^{2+} was used as the activating divalent. In addition, Ba^{2+}-evoked currents were blocked by the α7-specific antagonist MLA (Fig. 3, B and C). These results show that the divalent-activated currents were carried by the $K^{144}C/T^{198}C$ α7 AChR. Other mutations exhibited modest activation by Ba^{2+} (~ 10–15%, see Table 1), but the $K^{144}C/T^{198}C$ α7 AChR was the only phenotype in which divalents were full agonists. Divalents such as Zn^{2+}, Mg^{2+}, or Mn^{2+} did not elicit any current responses from the $K^{144}C/T^{198}C$ α7 AChR (data not shown), suggesting that the activation by divalent we observed is likely to be distinct from that reported for a recently cloned member of the cysteine-loop receptor gene family (Davies et al., 2003).

Divalent-Activated Currents Are Abolished by the $E^{172}Q$ Mutation. Previous studies showed that mutation of

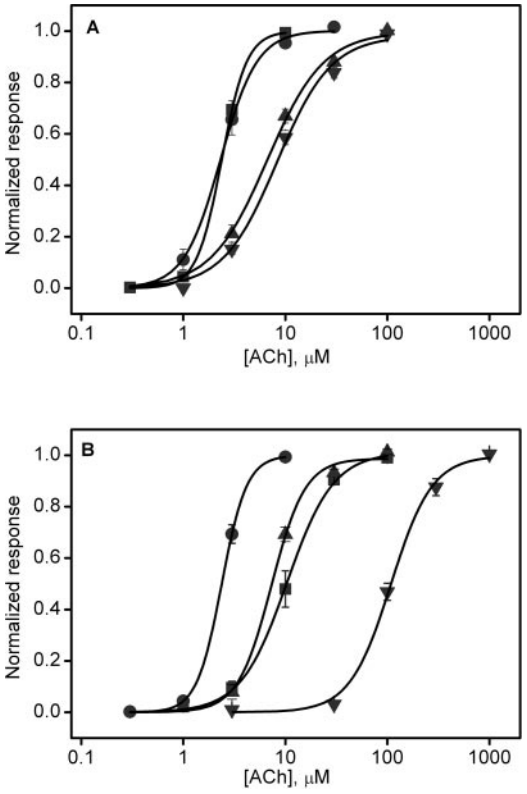

Fig. 2. Selected pairs of cysteine mutants express functional AChRs. A, ACh dose-response curves for $C^{115}A/L^{247}T$ background phenotype (●), $N^{142}C$ (▲), $T^{200}C$ (▼), and $T^{200}C/N^{142}C$ (■). B, $C^{115}A/L^{247}T$ (●), $K^{144}C$ (▲), $T^{198}C$ (▼), and $T^{198}C$ /$K^{144}C$ (■). Data are normalized to the maximal ACh current for each oocyte. Pairing of these cysteine mutants causes provides at least partial recovery from the effect of the single mutations. Additional data on these and other cysteine mutants are summarized in Table 1.

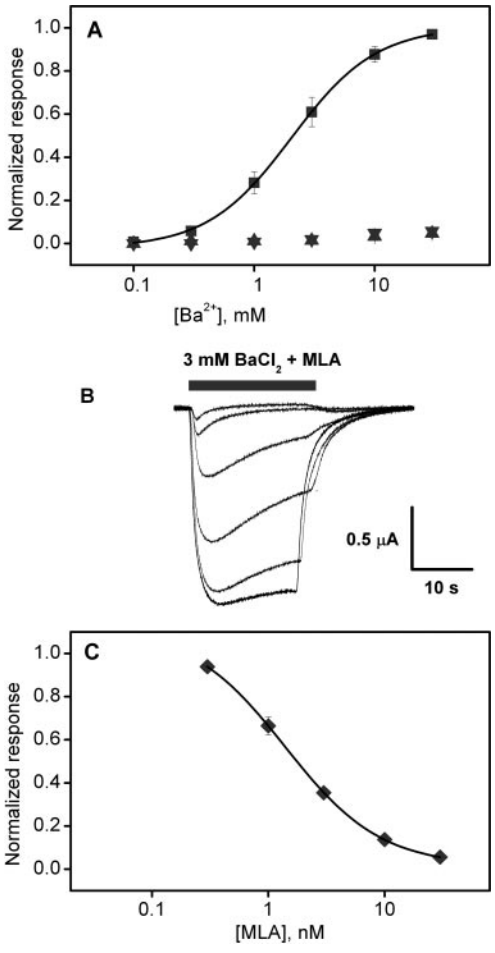

Fig. 3. Divalent cations activate α7 $K^{144}C/T^{198}C$ mutant receptors. The cysteine mutant pair $K^{144}C/T^{198}C$, when expressed in the $L^{247}T$ background, responds to bath-applied Ba^{2+} with currents similar to those observed in response to ACh. A, barium dose-response curve for $K^{144}C/T^{198}C$ (■). Neither of two single cysteines $K^{144}C$ (▲) or $T^{198}C$ (▼) show a similar response. Ba^{2+}-evoked currents are normalized to the maximal ACh-evoked current of each receptor type. B, responses of $K^{144}C/T^{198}C$ α7 receptors to 3 mM Ba^{2+} plus increasing concentrations of the α7-specific antagonist MLA. Blockade by MLA demonstrates that the Ba^{2+}-evoked currents were due to activation of α7 AChRs. C, MLA inhibition plotted from fractional peak currents, as shown in B, yields an apparent IC_{50} value of 1.4 nM, comparable with inhibition observed for ACh-evoked currents.

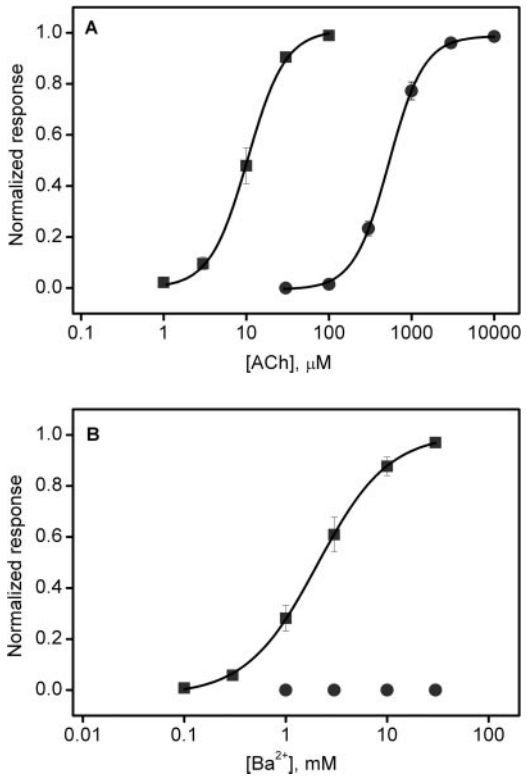

Fig. 4. Activation of $K^{144}C/T^{198}C$ by Ba^{2+} requires the conserved glutamate Glu^{172}. Neutralization of the charge at Glu^{172} shifts the ACh dose-response curve but eliminates activation by Ba^{2+}. Normalized dose response relationships to ACh (A) or Ba^{2+} (B) for $K^{144}C/T^{198}C$ (■) and $K^{144}C/T^{198}C/E^{172}Q$ (●). Currents are normalized to peak responses of each receptor type to a maximal dose of ACh.

the conserved glutamate at 172 eliminated divalent modulation of α7 AChRs, demonstrating that this residue is a critical component of a divalent allosteric binding site (Galzi et al., 1996; Eddins et al., 2002a). To test whether this site was involved in the activation by divalent cations of $K^{144}C/T^{198}C$ α7 AChR, we constructed α7 receptors with Glu^{172} mutated to glutamine in addition to $K^{144}C$ and $T^{198}C$ mutations. This construct displays an ACh dose-response relationship similar to that seen previously in the $E^{172}Q$ mutant (Eddins et al., 2002b) but shows no divalent-activated current (Fig. 4). This result suggests that the introduction of the $K^{144}C/T^{198}C$ cysteine pair enhances the endogenous allosteric modulation such that divalent binding to $K^{144}C/T^{198}C$ α7 receptors can induce the conformational changes necessary for channel opening even in the absence of cholinergic agonists.

The $K^{144}C/T^{198}C$ Mutant Pair Alters Wild-Type Divalent Modulation. The modulation of wild-type α7 AChRs by divalent cations includes a 2- to 3-fold decrease in the ACh EC_{50} value (Galzi et al., 1996). To test the potential importance of the β7/β9/β10 β-sheet in allosteric modulation of wild-type α7 AChRs, we examined the effects of divalent cations on the functional properties of $K^{144}C/T^{198}C$ mutant receptors in a normally desensitizing wild-type α7 AChR background. Figure 5A shows the modest enhancement of maximal ACh-evoked currents of wild-type α7 receptors elicited by addition of Ba^{2+}. Figure 5B shows that 10 mM Ba^{2+} also caused a decrease in the ACh EC_{50} value of wild-type α7 receptors. In contrast, the $K^{144}C/T^{198}C$ α7 receptors (in the wild-type background) show an absolute requirement for both divalent and ACh (Fig. 5, C and D). In the absence of added Ba^{2+}, maximal ACh-evoked currents were ~5% of

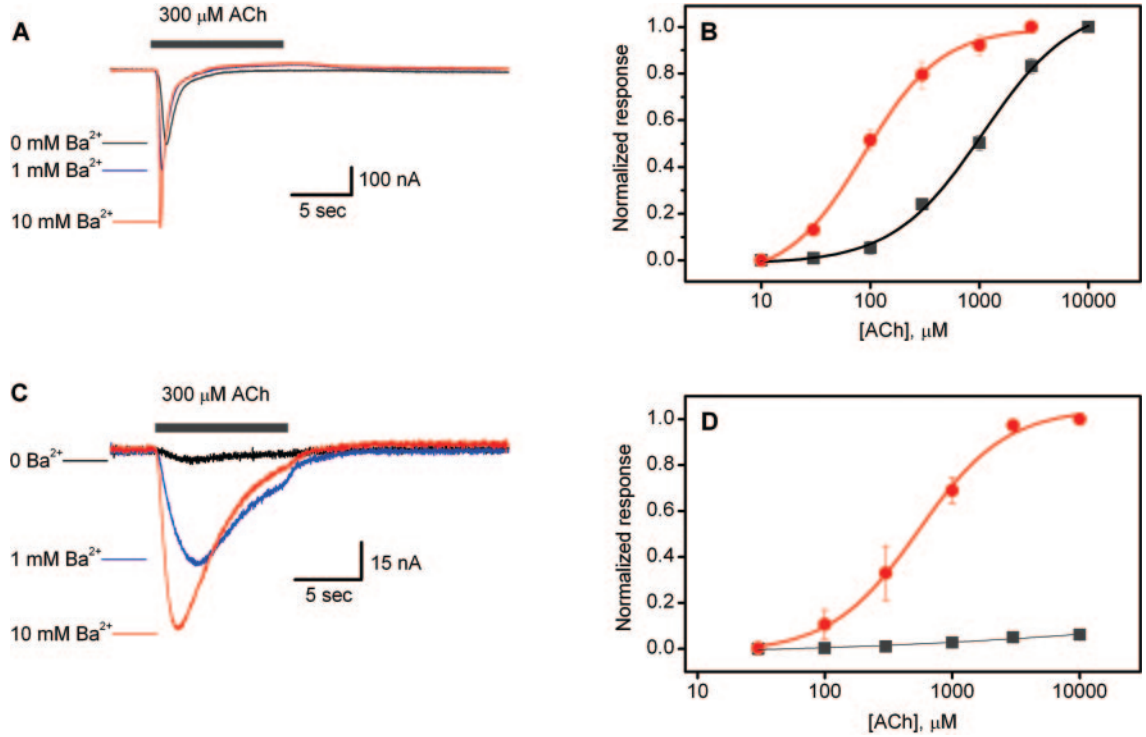

Fig. 5. Activation of $K^{144}C/T^{198}C$ in the wild-type background requires both ACh and divalent cations. A, current traces of wild-type α7 AChR (black) show potentiation by 1 mM (blue) or 10 mM (red) added Ba^{2+}. B, ACh dose-response curves in low divalent (0.1 mM Ca^{2+}, ■) and in 0.1 mM Ca^{2+} plus 10 mM Ba^{2+} (●, red). C, $K^{144}C/T^{198}C$ in a wild-type α7 background: divalent-evoked currents are no longer observed, and ACh-evoked currents are substantially diminished (black trace). Current responses for coapplication of ACh and 1 mM (blue trace) or 10 mM (red trace) Ba^{2+}. D, comparison of ACh dose responses in 0.1 mM Ca^{2+} (■) and 0.1 mM Ca^{2+} plus 10 mM Ba^{2+} (●, red) for $K^{144}C/T^{198}C$ in the wild-type α7 background.

maximal currents in ACh plus 10 mM Ba^{2+}. Thus, in $K^{144}C/T^{198}C$ α7 AChRs, divalents were coagonists required for the initiation of conformational changes leading to channel opening. Currents elicited by the combination of ACh and Ba^{2+} also displayed altered kinetics relative to wild-type α7 AChRs; the time constant for current decay increased ~4-fold, suggesting that the introduced cysteine pair slows channel desensitization and/or closing rates. These observations confirm the critical role of the β7/β9/β10 β-sheet in linking ACh binding and divalent modulation in the conformational changes responsible for gating the receptor channel.

Discussion

The goal of these experiments was to test the role of the outer β-sheet, formed by strands 7, 9, and 10, in the activation and allosteric modulation of α7 nicotinic receptors. The potential importance of this structural element was first suggested by its position between the ligand binding site and conserved regions near the transmembrane domain, such as the cysteine loop and the β1–β2 linker (Brejc et al., 2001). Based on the loss of sensitivity to thiol modifiers, we show that it is possible to introduce disulfide bonds between the β7 and β10 strands in at least two positions ($N^{142}C/T^{200}C$ and $K^{144}C/T^{198}C$) without a loss of ACh-evoked receptor activation. We also show that (in a nondesensitizing α7 variant) the putative disulfide bond between $K^{144}C$ and $T^{198}C$ enhances receptor activation by converting allosteric modulators (e.g., Ca^{2+} or Ba^{2+}) to full agonists.

Although the "modulation-activation" by divalent cations occurs around the conserved glutamate (Glu^{172}) of the β8–β9 linker, it also involves conformational transitions at the ligand binding site, because the competitive antagonist MLA prevents activation by divalent cations. This effect is specific for the Lys^{144} + Thr^{198} pair, suggesting that both the stabilization provided by a disulfide and its position in the outer β-sheet contribute to the phenotype. Our results are relevant to several recently proposed models for receptor activation and allow us to further refine hypotheses of the conformational transitions involved.

A report by Mukhtasimova et al. (2005) examined the role of several conserved residues surrounding agonist binding site in muscle AChRs, including the lysine homologous to α7 Lys^{144}. They used a combination of mutagenesis, single-channel electrophysiology, and ligand binding experiments to demonstrate an interdependence between Lys^{144}, a C-loop tyrosine (Tyr^{187} in α7), and the conserved aspartate in β10 (Asp^{196}). They proposed a "salt-bridge switch" model in which a salt bridge between Lys^{144} and Asp^{196} is present in the absence of ligand. In this model, the binding of ACh leads to a contraction of the C-loop and moves Tyr^{187} close to Lys^{144}, where it replaces the Asp^{196} and forms a new salt bridge. Our findings that a covalent bond between substituted cysteine residues at positions Lys^{144} and Thr^{198} can exist in a receptor that is ACh-activated seems incompatible with this model. This discrepancy may arise from the differences in the AChR isoforms used in each study, because the α1 subunit of muscle shows significant sequence differences, particularly in the C loop, compared with the α7 AChR. It is likely that such differences will reflect variations in the subtle conformational changes underlying the activation of each receptor isoform.

Current models place the binding site for divalent cations at the interface between adjacent subunits, at which several conserved charged residues are found in close proximity (Le Novere et al., 2002). In addition to Glu^{172}, the binding site may include the conserved glutamate (Glu^{44}) and aspartates (Asp^{41} and Asp^{43}) that structural models place in the region linking β1 and β2, the two major β strands of the "inner" β-sheet. Several recently proposed models for receptor activation have suggested a role for the β1–β2 linker in the coupling of ligand binding to receptor activation (Kash et al., 2004; Law et al., 2005; Lee and Sine, 2005). A common theme in these proposed mechanisms is an interaction between components of the extracellular domain and the amino acid residues linking the second and third transmembrane helices (the M2–M3 linker). Our results suggest that the outer β-sheet plays a role in transmitting the conformational transitions at the binding site to this or other mediators of channel gating.

Law et al. (2005) used molecular dynamics to model the gating of the human α7 receptor. They constructed a model using LBD coordinates from the ACh binding protein (Brejc et al., 2001) and ICD coordinates from *T. californica* AChR cryoelectron microscopy (Miyazawa and Unwin, 2003). They noted both outward motions of the C loop (corresponding to a relaxation to the closed state) and asymmetric movement of the transmembrane domains consistent with channel closing. Based on these observations, they suggest that in the process of activation, the outer β-sheet transmits the gating signal from the binding site to the ICD via contacts with the conserved cysteine loop at the N-terminal of β7. Our data provide experimental evidence to support this model and allow us to propose a mechanism for the allosteric action of divalent cations in the process of AChR activation.

We found that introduction of a disulfide at a central location in the outer β-sheet allowed divalent binding at one end of the sheet (the "bottom") to elicit the same conformational transition that agonist binding did at the other end (the "top"). This suggests that the outer β-sheet may act as a lever that moves, with the disulfide at or near the fulcrum. In this way, binding at one end can elicit the same pivoting motions as those elicited by binding at the other. Compounds such as MLA can prevent activation either by direct competition with ACh or by a noncompetitive mechanism, as suggested by Law et al. (2005). We can explain the effect of introducing the $K^{144}C/T^{198}C$ disulfide into the α7 wild type if we assume that the $L^{247}T$ mutation exerts a "relaxing" effect on the entire transduction pathway. In the $L^{247}T$ background, introducing the $K^{144}C/T^{198}C$ disulfide allows either ACh or divalent cations to exert enough leverage on the outer β-sheet to activate the channel. In the wild-type background, however, the stiffening of the outer β-sheet by the introduction of the $K^{144}C/T^{198}C$ disulfide creates a greater energetic barrier between closed and open states. This slows channel kinetics and leads to a requirement for binding of both ACh and divalent cations to efficiently drive the conformational transitions, leading to channel opening.

Lyford et al. (2003) provided evidence for an asymmetric rotation of subunits as part of agonist-evoked receptor activation. This is consistent with the model developed using molecular dynamics (Law et al., 2005) in which two subunits exhibit rotational motion during activation, but the others do not. Lee and Sine (2005) have proposed a more detailed

activation scheme for the *T. californica* AChR in which the coupling of the binding site to the channel is mediated by an electrostatic interaction between residues of the inner and outer β-sheets (Glu^{45} and Arg^{209}). The movement of the outer sheet we propose could represent a step in the activation pathway for the α7 AChR comparable with the Glu^{45} + Arg^{209} interaction in the *T. californica* AChR that serves to link the outer and inner β-sheets. It is noteworthy that the *T. californica* AChR does not show the same potentiation by divalent cations as the α7 AChR, and the conserved glutamate corresponding to the *T. californica* Glu^{45} in α7 (Glu^{44}) is has been shown to participate in a formation of the divalent binding site (Galzi et al., 1996). Thus, the difference in divalent modulation between the two isoforms may be due to distinct mechanistic roles for this conserved glutamate.

In another recent report, Lummis et al. (2005) showed data suggesting that activation of another cysteine-loop receptor (5-hydroxytryptamine type 3) may involve *cis-trans* isomerization of a proline residue in the M2–M3 loop. Because this residue is not conserved throughout the cysteine-loop receptor family, their result implies that there must be different activation mechanisms used by different receptor isoforms (Czajkowski, 2005). This is consistent with another recent report showing that whereas electrostatic interactions are key to the movements linking binding and gating, these interactions are mediated by different sets of residues in different receptor isoforms (Xiu et al., 2005). Our results provide evidence for a critical role of the outer β-sheet in the conformational mechanism linking agonist binding to channel gating in the α7 AChR. They also suggest, compared with other recent studies, that various AChR isoforms use different conformational transitions in the coupling of ligand binding to channel activation.

References

Brejc K, van Dijk WJ, Klaassen RV, Schuurmans M, van Der Oost J, Smit AB, and Sixma TK (2001) Crystal structure of an ACh-binding protein reveals the ligand-binding domain of nicotinic receptors. *Nature (Lond)* **411:**269–276.

Celie PH, Klaassen RV, van Rossum-Fikkert SE, van Elk R, van Nierop P, Smit AB, and Sixma TK (2005a) Crystal structure of acetylcholine-binding protein from *Bulinus truncatus* reveals the conserved structural scaffold and sites of variation in nicotinic acetylcholine receptors. *J Biol Chem* **280:**26457–26466.

Celie PH, van Rossum-Fikkert SE, van Dijk WJ, Brejc K, Smit AB, and Sixma TK (2005b) Nicotine and carbamylcholine binding to nicotinic acetylcholine receptors as studied in AChBP crystal structures. *Neuron* **41:**907–914.

Czajkowski C (2005) Neurobiology: triggers for channel opening. *Nature (Lond)* **438:**167–168.

Davies PA, Wang W, Hales TG, and Kirkness EF (2003) A novel class of ligand-gated ion channel is activated by Zn^{2+}. *J Biol Chem* **278:**712–717.

Eddins D, Lyford LK, Lee JW, Desai SA, and Rosenberg RL (2002a) Permeant but not impermeant divalent cations enhance activation of non-desensitizing $alpha_7$ nicotinic receptors. *Am J Physiol* **282:**C796–C804.

Eddins D, Sproul AD, Lyford LK, McLaughlin JT, and Rosenberg RL (2002b) Glutamate 172, essential for modulation of $L^{247}T$ alpha7 ACh receptors by Ca^{2+}, lines the extracellular vestibule. *Am J Physiol* **283:**C1454–C1460.

Galzi JL, Bertrand S, Corringer PJ, Changeux JP, and Bertrand D (1996) Identification of calcium binding sites that regulate potentiation of a neuronal nicotinic acetylcholine receptor. *EMBO (Eur Mol Biol Organ) J* **15:**5824–5832.

Grosman C, Zhou M, and Auerbach A (2000) Mapping the conformational wave of acetylcholine receptor channel gating. *Nature (Lond)* **403:**773–776.

Holmgren M, Liu Y, Xu Y, and Yellen G (1996) On the use of thiol-modifying agents to determine channel topology. *Neuropharmacology* **35:**797–804.

Horenstein J, Wagner DA, Czajkowski C, and Akabas MH (2001) Protein mobility and GABA-induced conformational changes in $GABA_A$ receptor pore-lining M2 segment. *Nat Neurosci* **4:**477–478.

Karlin A (2002) Emerging structure of the nicotinic acetylcholine receptors. *Nat Rev Neurosci* **3:**102–114.

Karlin A and Akabas MH (1998) Substituted-cysteine accessibility method. *Methods Enzymol* 293:123–145.

Kash TL, Kim T, Trudell JR, and Harrison NL (2004) Evaluation of a proposed mechanism of ligand-gated ion channel activation in the $GABA_A$ and glycine receptors. *Neurosci Lett* **371:**230–234.

Law RJ, Henchman RH, and McCammon JA (2005) A gating mechanism proposed from a simulation of a human alpha7 nicotinic acetylcholine receptor. *Proc Natl Acad Sci USA* **102:**6813–6818.

Lee WY and Sine SM (2005) Principal pathway coupling agonist binding to channel gating in nicotinic receptors. *Nature (Lond)* **438:**243–247.

Le Novere N, Grutter T, and Changeux JP (2002) Models of the extracellular domain of the nicotinic receptors and of agonist- and Ca^{2+}-binding sites. *Proc Natl Acad Sci USA* **99:**3210–3215.

Lester HA, Dibas MI, Dahan DS, Leite JF, and Dougherty DA (2004) Cys-loop receptors: new twists and turns. *Trends Neurosci* **27:**329–336.

Lummis SC, Beene DL, Lee LW, Lester HA, Broadhurst RW, and Dougherty DA (2005) Cis-trans isomerization at a proline opens the pore of a neurotransmitter-gated ion channel. *Nature (Lond)* **438:**248–252.

Lyford LK, Sproul AD, Eddins D, McLaughlin JT, and Rosenberg RL (2003) Agonist-induced conformational changes in the extracellular domain of α7 nicotinic acetylcholine receptors. *Mol Pharmacol* **64:**650–658.

Miyazawa A, Fujiyoshi Y, and Unwin N (2003) Structure and gating mechanism of the acetylcholine receptor pore. *Nature (Lond)* **423:**949–955.

Mukhtasimova N, Free C, and Sine SM (2005) Initial coupling of binding to gating mediated by conserved residues in the muscle nicotinic receptor. *J Gen Physiol* **126:**23–39.

Revah F, Bertrand D, Galzi JL, Devillers-Thiery A, Mulle C, Hussy N, Bertrand S, Ballivet M, and Changeux JP (1991) Mutations in the channel domain alter desensitization of a neuronal nicotinic receptor. *Nature (Lond).* **353:**846–849.

Sine SM (2002) The nicotinic receptor ligand binding domain. *J Neurobiol* **53:**431–446.

Sullivan DA and Cohen JB (2000) Mapping the agonist binding site of the nicotinic acetylcholine receptor. Orientation requirements for activation by covalent agonist. *J Biol Chem* **275:**12651–12660.

Unwin N (2005) Refined structure of the nicotinic acetylcholine receptor at 4A resolution. *J Mol Biol* **346:**967–989.

Xiu X, Hanek AP, Wang J, Lester HA, and Dougherty DA (2005) A unified view of the role of electrostatic interactions in modulating the gating of cys loop receptors. *J Biol Chem* **280:**41655–41666.

Address correspondence to: Dr. James T. McLaughlin, Department of Pharmacology, CB# 7365, University of North Carolina at Chapel Hill, Chapel Hill, NC 27599-7365. E-mail: jmclaughlin@unc.edu